Turkish Journal of Chemistry

http://journals.tubitak.gov.tr/chem/

Research Article

Turk J Chem
(2017) 41: 381 – 390

doi:10.3906/kim-1608-53

Fabrication of multilayer graphene oxide-reinforced high density polyethylene nanocomposites with enhanced thermal and mechanical properties via thermokinetic mixing

Burcu SANER OKAN*
Sabancı University Nanotechnology Research and Application Center, İstanbul, Turkey
Sabancı University Integrated Manufacturing Technologies Research and Application Center
& Composite Technologies Center of Excellence, İstanbul, Turkey

Received: 25.08.2016 • **Accepted/Published Online:** 27.11.2016 • **Final Version:** 16.06.2017

Abstract: High density polyethylene (HDPE) was compounded with thermally exfoliated graphene oxide (TEGO) by thermokinetic mixing in a short time. High shear rates during the compounding process provided high exfoliation and proper dispersion of graphene layers in the polymer matrix. Different TEGO/polymer ratios were used to get efficient melt mixing. Structural analysis by spectroscopic techniques confirmed the exfoliation of TEGO sheets and the coverage of their surfaces by HDPE chains. Furthermore, homogeneous dispersion of graphene sheets in the matrix led to the enhancement in the mechanical and thermal properties of HPDE-based nanocomposites. Especially stress concentration sites were significantly reduced by preventing the agglomeration and restacking of graphene sheets in the matrix. Therefore, the tensile modulus and strength of HDPE nanocomposite increased about 36.5% and 45.7%, respectively, with the incorporation of 2 wt% TEGO. Microscopy analysis showed the separation of graphene layers in the cross-sectional area of composite specimens. TEGO-reinforced HDPE nanocomposites showed high thermal stability compared to the neat sample.

Key words: Graphene, high density polyethylene, nanocomposite, compounding, melt mixing, exfoliation

1. Introduction

High density polyethylene (HDPE) is a widely used thermoplastic polymer because of its low cost, ease of recycling, good processability, nontoxicity, biocompatibility, and good chemical resistance. Neat HDPE polymer does not meet industrial demands; the properties of stiffness and rigidity need to be improved. Several fillers such as carbon nanotubes,[1] graphene,[2] natural fiber,[3] clay,[4] and carbon black are used to improve the characteristic properties of HDPE polymer. Among these fillers, graphene has attracted great attention due to its superior physical, chemical, and electrical properties and its 2-dimensional structure in various applications including composites, batteries, capacitors, biosensors, and electronic devices and other material innovations.[5] There are several methods for the production of graphene layers. A widely used technique is chemical exfoliation of graphene sheets from graphite flakes by applying oxidation and thermal expansion.[6] The type of graphene synthesized by applying this chemical technique is widely used in the fabrication of structural materials and as a reinforcing agent in the chosen matrix.[7] The dispersion of graphene in the polymer matrix is a challenging step in the production of graphene-reinforced polymer composites. Therefore, the surface chemistry of graphene and

*Correspondence: bsanerokan@sabanciuniv.edu

its surface functional groups is of significant importance to obtain an ideal composite structure by providing better interactions between graphene and the polymer matrix.[8]

In the literature, there are various attempts regarding the utilization of graphene as a reinforcing agent in HDPE to attain high performance composite materials. For instance, Guo et al.[9] enhanced the thermal stability and flame retardancy of HPDE composites by reinforcing fullerene decorated graphene oxide (GO). Li et al.[10] demonstrated an increase in the tensile modulus of HDPE/expanded graphite composites with increasing filler content (up to 70 vol%) whereas their tensile strength values decreased. In another work, Wei et al.[2] produced graphene/HDPE composites with improved elongation at break, impact strength, and yield strength by solid state shear milling methods at room temperature by different graphene loadings changing from 0.1 wt% to 2 wt%. Furthermore, when HDPE was compounded with 15 vol% graphene nanoplatelets coated by wax to improve the dispersion, the flexural strength of HDPE composite was improved up to $\sim$116%.[11,12] However, this high loading can cause severe aggregations during compounding and increase stress concentration sites in composites. In order to improve the dispersion of graphene in the HDPE matrix, graphene flakes were exfoliated in toluene with recycled HDPE before the compounding process and the ultimate tensile strength and elastic modulus of the composite with 4 wt% graphene content were improved about 56% and 117%, respectively.[13] Herein, graphene sheets were exfoliated in toxic solvents such as xylene and toluene to increase its dispersion and compatibility with the HDPE matrix. Moreover, surface treatments lead to the additional steps in composite production and thus an increase in production cost in scaling-up. Wang et al.[14] treated the surface of GO with glycidyl trimethyl ammonium chloride and produced HDPE/nylon composite by in situ polymerizations using 0.02 wt% of GO. The tensile strength, elongation at break, impact strength, and compressive strength of this resultant composite were enhanced by 14.7%, 21.0%, 30.0%, and 27.2%, respectively. Therefore, there are several parameters such as type of graphene material, its production technique, and the amount of oxygen functional groups in the graphene structure that directly affect the mechanical, thermal, and electrical properties of polymeric composites.

In the present study, thermally exfoliated graphene oxide (TEGO) used as a reinforcing agent was obtained by thermal exfoliation resulting in the removal of most of functional groups from the structure and thus the control of surface chemistry.[15] TEGO was mixed with HDPE by Gelimat thermokinetic mixer under high shear rates at different TEGO/polymer ratios. The proposed compounding process occurred in one step without applying any pre- and posttreatments and hence quickened the manufacturing of composites and reduced the environmental risks coming from toxic chemicals. In order to get high performance graphene based composite, structural, thermal, and morphological analyses were conducted for various TEGO amounts ranging from 0.5 wt% to 2 wt%. The optimum TEGO amount in HDPE polymer was determined based on tensile tests of specimens. High shear rate is a critical issue to attain homogeneous dispersion of graphene layers through polymer chains and prevent the agglomeration of graphene sheets and thus the failures of composites. Microscopic analysis in fractured surfaces provided an understanding of graphene distribution in the polymer matrix after failures.

2. Results and discussion

2.1. Structural analysis of TEGO-reinforced HDPE nanocomposites

In order to understand the interactions of graphene sheets with HDPE polymer chains, the changes in functional groups were analyzed by Fourier transform infrared spectroscopy (FTIR) as seen in Figure 1. The characteristic peaks at around 2910 cm^{-1} and 2845 cm^{-1} belong to CH_2 asymmetric and symmetric stretching frequen-

cies, respectively.[16] The peaks at 1460 cm^{-1} and 716 cm^{-1} are related to bending and rocking deformations, respectively.[16] The peaks at 1650 cm^{-1} and 1580 cm^{-1} belonging to C=O and C=C aromatic bonds, respectively, became intense with the addition of TEGO sheets to the polymer matrix. This indicates the presence of graphene sheets in the polymer matrix after the compounding process.

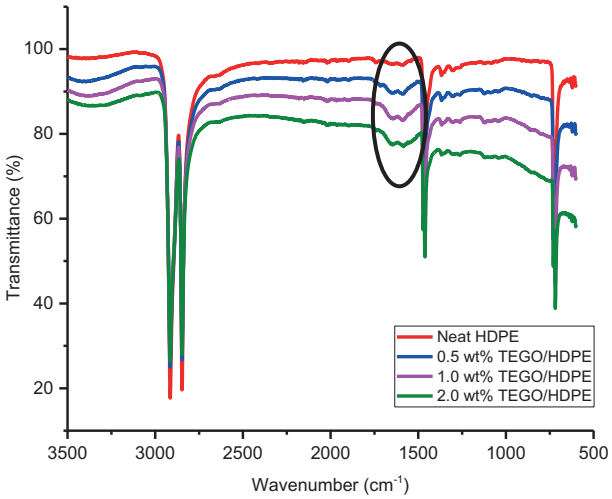

Figure 1. FTIR spectra of neat HDPE and TEGO-reinforced HDPE composites with different TEGO loadings.

Raman spectroscopy is an efficient technique to analyze graphene sheets and determine the number of graphene layers and measure the defects in the structure. Figure 2 exhibits the Raman spectra of TEGO, neat HDPE, and 2 wt% TEGO-reinforced HDPE specimens. TEGO has three main characteristic peaks, which are a D band at 1360 cm^{-1} related to the amount of defects in the structure, and G and 2D bands at around 1580 cm^{-1} and 2700 cm^{-1} that change in shape, position, and relative intensity with the number of graphene layers.[17] D, G, and 2D bands appear in the Raman spectrum of TEGO-reinforced HDPE nanocomposite when compared to the Raman spectrum of neat HDPE as seen in Figure 2.

HDPE is a semicrystalline polymer. Figure 3 shows the X-ray diffraction (XRD) patterns of TEGO, neat HDPE, and 2 wt%/TEGO composites. Two peaks at $2\theta = 21°$ and $2\theta = 23.5°$ correspond to 110 and 200 reflections of HDPE polymer.[18] TEGO has a 002 peak at around $2\theta = 26.5°$. After the integration of graphene sheets through polymer chains, a 002 peak belonging to TEGO is seen in the XRD spectrum of HDPE composite and the intensity of the HDPE's peaks decreases. Structural characterization supports the incorporation of TEGO sheets through HDPE polymer chains during the compounding process.

2.2. Thermal behaviors of TEGO-reinforced HDPE composites

Figure 4 exhibits thermal gravimetric analysis (TGA) curves of HDPE nanocomposites with different TEGO loadings under N_2 atmosphere. The degradation curves showed that neat HDPE specimen starts to lose weight at around 230 °C, whereas HDPE containing TEGO sheets can preserve thermal stability up to 300 °C and then they start to degrade. There is a gradual increase in thermal stability observed with increasing TEGO amount. This means that TEGO increases the thermal degradation temperatures of composite specimens. Table 1 gives the summary of weight loss temperatures of composite specimens.

In addition, differential scanning calorimeter (DSC) analysis was performed to examine the changes in melting point and crystallization temperatures of specimens as a function of graphene content. Figure 5

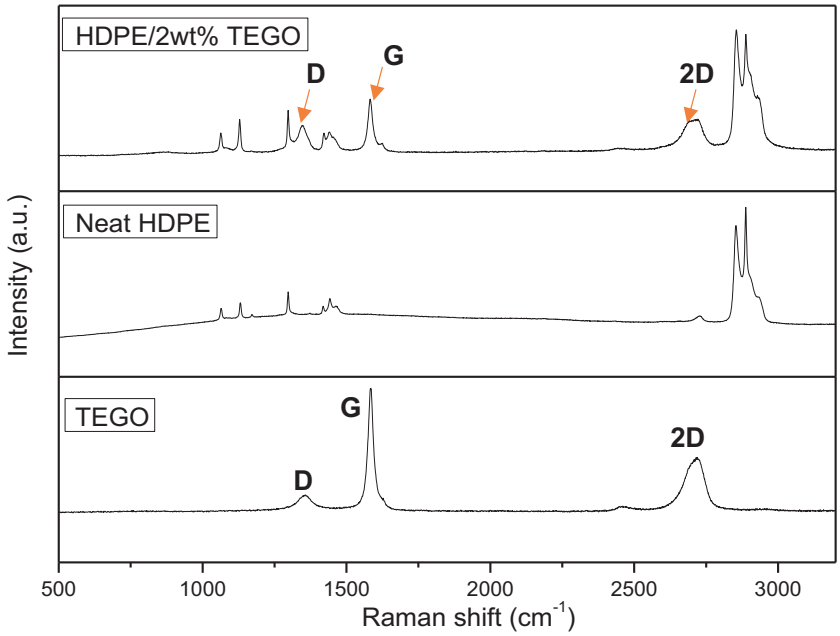

Figure 2. Raman spectra of TEGO, neat HDPE, and 2 wt% TEGO-reinforced HDPE nanocomposite.

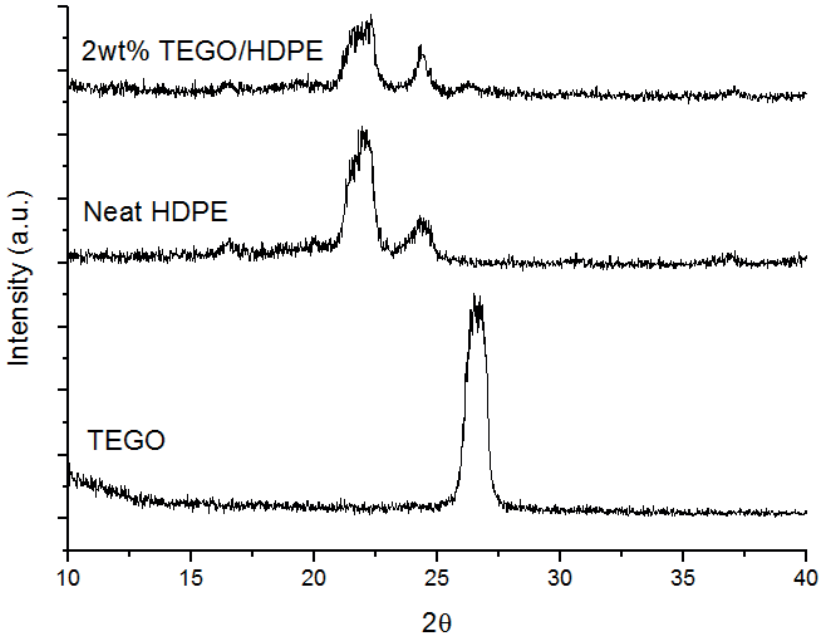

Figure 3. XRD spectra of TEGO, neat HDPE, and 2 wt% TEGO/HDPE nanocomposite.

represents DSC 1st heating and cooling curves of composites. In the 1st heating cycles seen in Figure 5a, melting temperatures of HDPE composites decrease with the integration of TEGO sheets since graphene sheets cause heterogeneous nucleation and the formation of crystalline regions by changing the arrangement of polymer chains.[2] In the cooling cycles shown in Figure 5b, crystallization temperature (Tc) increases with the addition of TEGO in the polymer matrix due to the random dispersion of restacked graphene sheets and the limitations

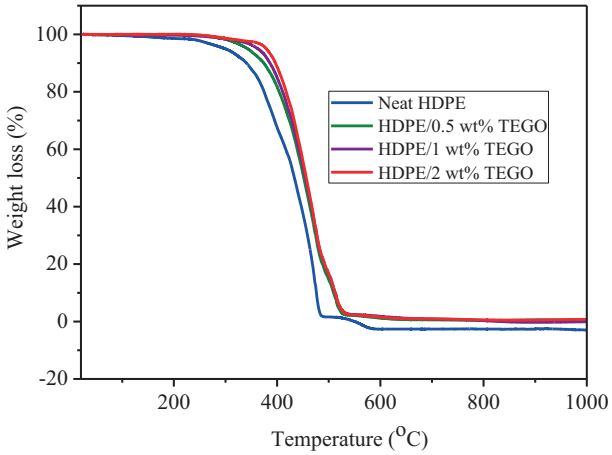

Figure 4. TGA curves of neat HDPE and TEGO-reinforced HDPE composites with different amounts of TEGO.

Table 1. Initial weight loss temperatures of TEGO-reinforced HDPE composites.

Specimen type	Initial weight loss temperature (°C)
Neat HDPE	230
0.5 wt% TEGO/HDPE	305
1 wt% TEGO/HDPE	315
2 wt% TEGO/HDPE	320

in the mobility of polymer chains through TEGO layers.[2] Moreover, the high surface area of graphene sheets enables these chains to act as a nucleating agent and thus increase crystallization at high temperatures.[19] However, there is no significant difference in Tc values of 0.5 wt%, 1 wt%, and 2 wt% TEGO-reinforced composites. This stems from less variation in the crystal size of materials.[20] Table 2 summarizes melting and crystallization temperatures of neat and TEGO-reinforced HDPE composites.

Table 2. Melting and crystallization temperatures of neat and TEGO-reinforced HDPE nanocomposites.

Sample	T_m (°C)	Tc (°C)
Neat HDPE	144.2	116.5
0.5 wt% TEGO/HDPE	143.3	120.8
1 wt% TEGO/HDPE	137.7	120.3
2 wt% TEGO/HDPE	138.1	120.2

2.3. Mechanical behaviors of HPDE nanocomposites with different TEGO loadings

The 4% oxygen functional groups of TEGO trigger the blending process between graphene layers and polymer chains. In order to get an ideal structure and prevent defects and reduce stress concentrations, it is important to distribute the graphene layers in the structure. Therefore, thermokinetic mixing has a significant role to separate graphene layers by breaking down Van der Waals forces between these layers and prevents their restacking under high shear rates and also increases the diffusion of polymer chains through graphene sheets and covers their surfaces by providing sufficient temperature. Stress–strain curves of HDPE nanocomposites reinforced by different TEGO amounts ranging between 0.5 wt% and 2 wt% are shown in Figure 6. The stress–strain curves show a stiff initial response at strain values up to ∼15 % and there is linearity between stress and strain. The modulus and strength values of HDPE composite are enhanced about 36.5% and 45.7%, respectively, by the

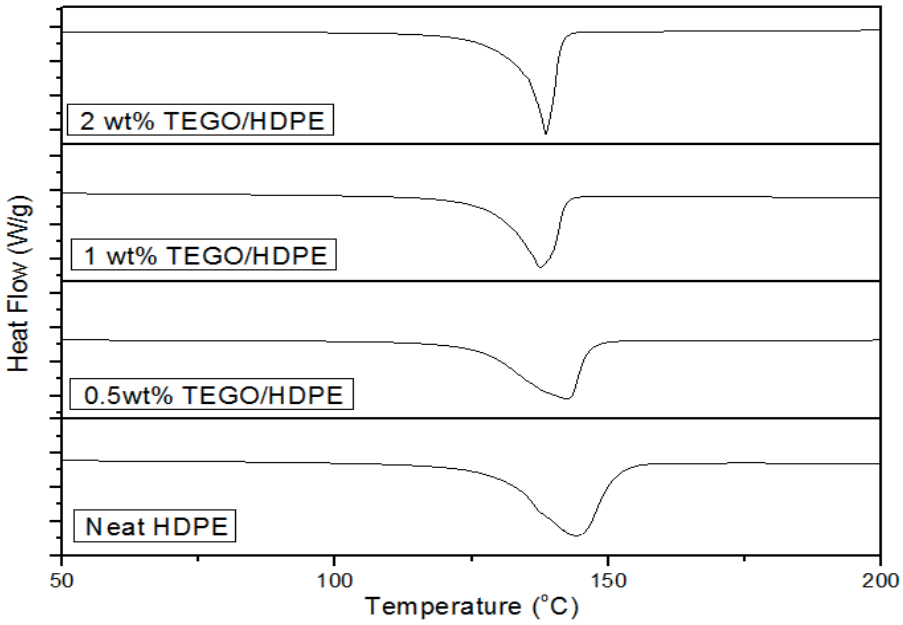

(a)

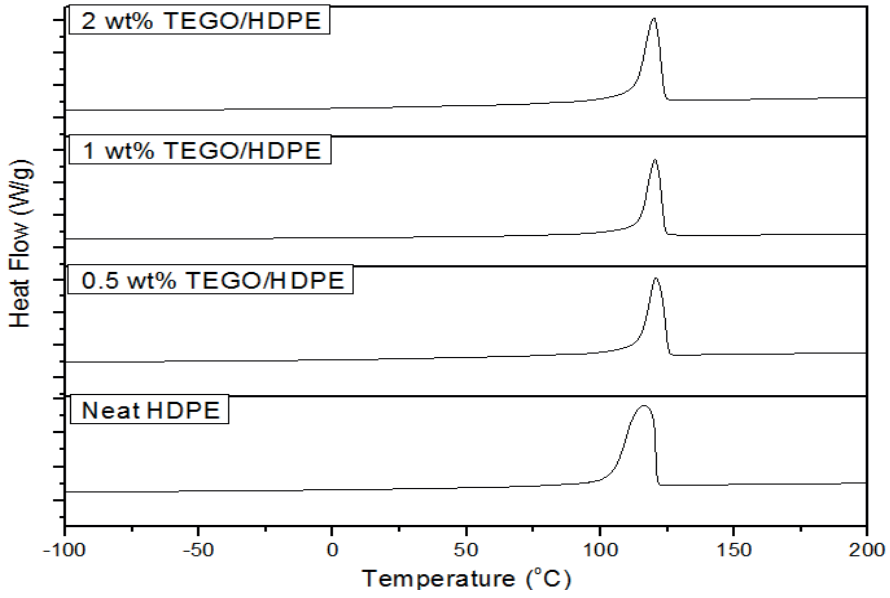

(b)

Figure 5. DSC curves of neat HDPE and TEGO-reinforced HDPE nanocomposites (a) 1st heating cycle and (b) cooling cycle.

addition of 2% TEGO. This specimen also showed a significant reduction at the strain of 18% and it was broken down as seen in Figure 6. However, the other specimens reinforced by 0.5 wt% and 1 wt% were elongated up to the stain values of 60% and 95%, respectively. When we looked at the neat specimen, it was elongated up to the strain of 170%. This indicates that the materials become more crystalline with the addition of TEGO sheets and the orientations of polymer chains decrease dramatically due to the dispersion of graphene layers. Table 3 summarizes the modulus and strength improvement percentages of HDPE composites.

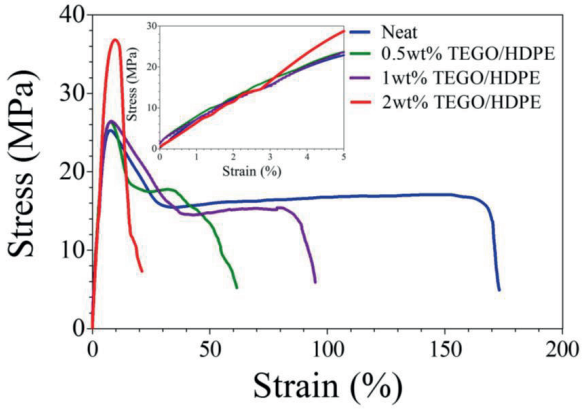

Figure 6. Tensile stress–strain curves of neat HDPE and TEGO-reinforced HDPE composites with different TEGO loadings.

Table 3. Improvement percentages of TEGO-reinforced HDPE nanocomposites.

TEGO amount	0.5 wt%	1 wt%	2 wt%
Modulus improvement (%)	16.5	12.9	36.5
Strength improvement (%)	14.8	6.9	45.7

2.4. Fracture analysis by SEM and TEM

Figures 7a and 7b show scanning electron microscopy (SEM) images of as-received TEGO samples at different magnifications. TEGO sheets have a worm-like structure after oxidation and thermal exfoliation. Surface morphologies in the fractured area provide an understanding of the dispersion behavior of graphene in the matrix. Figure 8 exhibits SEM images of the freeze-fractured surfaces of neat and graphene-reinforced specimens. In Figure 8a, the neat specimen has a rough surface but after the integration of graphene sheets in the structure the fractured surface becomes smooth as seen in Figure 8b. Transmission electron microscopy (TEM) images in Figures 9a–9c show the separation of graphene layers and their homogeneous distribution in the matrix at different magnifications. This indicates the complete wetting of reinforcement sheets by the polymer matrix.

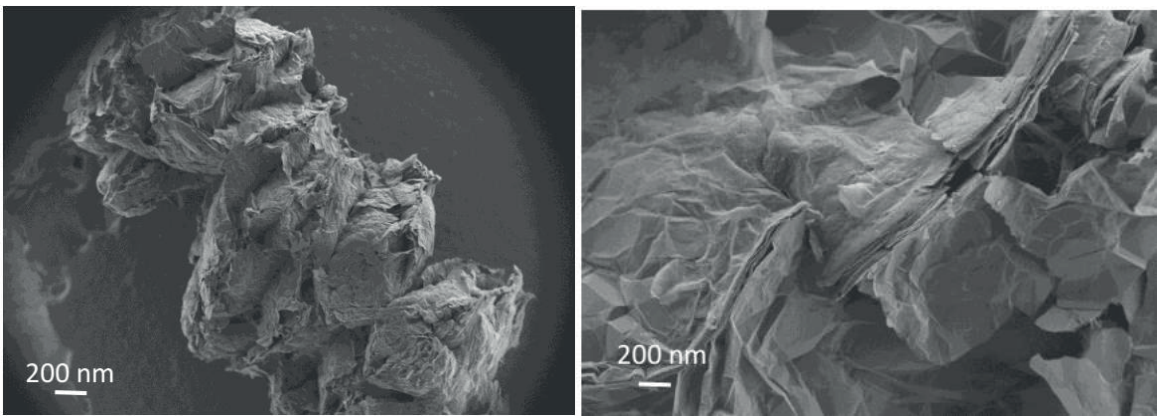

Figure 7. SEM images of TEGO sheets at different magnifications.

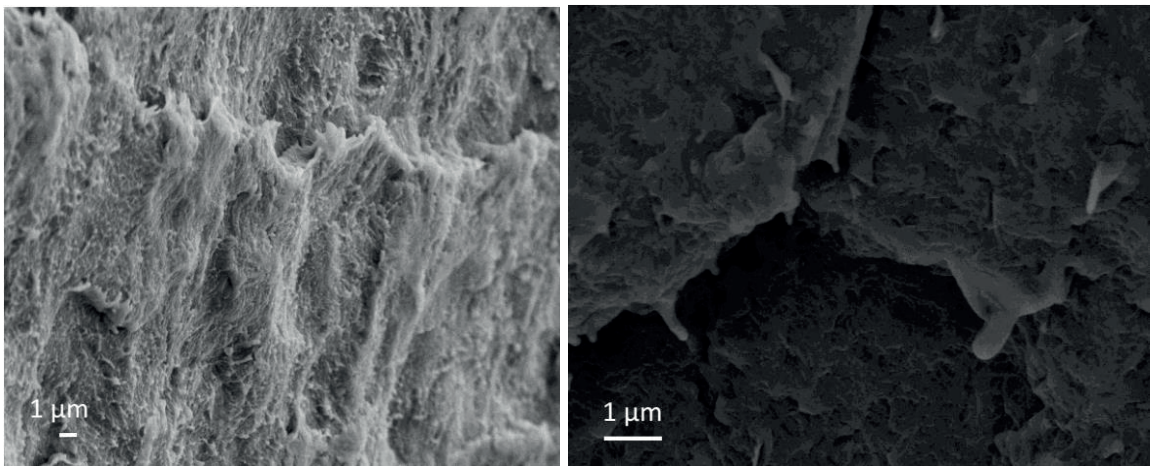

Figure 8. SEM images of freeze-fractured surfaces of (a) neat HDPE and (b) 2 wt% TEGO/HDPE nanocomposites.

3. Experimental

3.1. Materials

TEGO-Grade 1 was received from NANOGRAFEN Co. TEGO has approximately 4% surface oxygen groups and an average number of 25 graphene layers that is calculated by using Debye–Scherrer equations and its BET surface area is about 11 m^2/g. SABIC-High density polyethylene (HDPE)-B-UP 8016-16 was used for compounding experiments.

3.2. Composite production

TEGO was mixed with HDPE by custom-made Gelimat thermokinetic mixing/compounding machine at shear rate of 5500 rpm at 215 °C for 45 s. TEGO loadings were adjusted as 0.5, 1, and 2 wt%.

3.3. Characterization

The changes in the functional groups of graphene-based samples were detected by Netzsch FTIR. Thermal properties of samples were determined by Shimadzu TGA and TA Q2000 modulated DSC at a scanning rate of 10 °C/min under nitrogen atmosphere. Structural changes in graphene-based samples were analyzed by Renishaw InVia Reflex Raman Microscopy System between 100 and 3500 cm^{-1}. Cross-sectional analysis of graphene specimens was done by a Leo Supra 35VP Field Emission SEM and JEOL 2100 Lab6 High Resolution TEM. Dog-bone-shaped composite specimens for tensile tests were prepared by DSM injection molding machine. Mechanical behaviors of specimens were investigated by ZWICK Proline 100 Universal Test Machine (UTM) with 10 kN load cell at constant cross-head speed of 20 mm/min.

4. Conclusions

Graphene sheets were distributed homogeneously through HDPE polymer chains by thermokinetic mixing at solid state under high shear rates. Their distribution behavior affected the mechanical performance in a positive manner. Modulus and tensile strength values were enhanced by 36.5% and 45.7%, respectively, by the incorporation of 2 wt% TEGO. TEGO consists of graphene layers in a hexagonal arrangement bonded together by weak van der Waals forces. These layers were broken down during the compounding process by thermokinetic mixer under high shear rates and thus polymer chains can diffuse easily through graphene layers and cover their

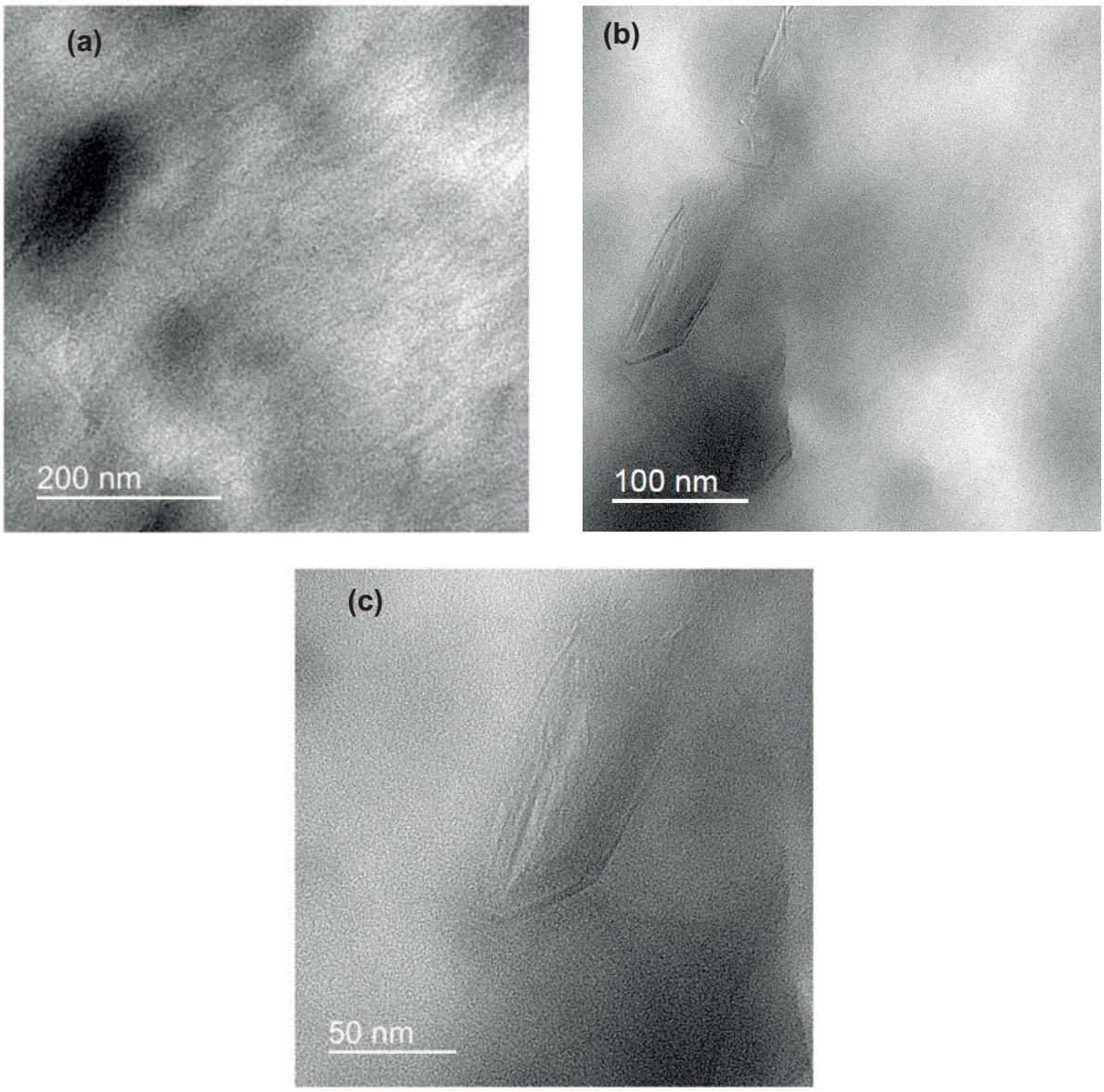

Figure 9. (a), (b), and (c) TEM images of cross-sectional area of HDPE nanocomposite with 2 wt% TEGO loading at different magnifications.

surfaces. Therefore, modulus and strength improvement values indicated good dispersion of graphene layers in the HDPE matrix. SEM and TEM techniques also confirmed this uniform distribution in the fractured surfaces of composites. Structural analysis by Raman spectroscopy and XRD indicated the presence of graphene sheets in the polymer matrix. The thermal degradation properties of HDPE nanocomposites were also improved by the addition of TEGO due to the high thermal stability of graphene sheets. Consequently, thermokinetic mixing, which is a feasible and cost-effective process, speeds up large-scale production of nanomaterial-reinforced polymeric masterbatches and opens up new opportunities in the plastic industry.

References

1. Zou, Y. B.; Feng, Y. C.; Wang, L.; Liu, X. B. *Carbon* **2004**, *42*, 271-277.
2. Wei, P. F.; Bai, S. B. *RSC Adv.* **2015**, *5*, 93697-93705.
3. Mendes, L. C.; Cestari, S. P. *Mater. Sci. Appl.* **2011**, *02*, 1331-1339.
4. Pegoretti, A.; Dorigato, A.; Penati, A. *Express Polym. Lett.* **2007**, *1*, 123-131.
5. Geim, A. K. *Science* **2009**, *324*, 1530-1534.
6. Saner, B.; Okyay, F.; Yurum, Y. *Fuel* **2010**, *89*, 1903-1910.
7. Zanjani, J. S. M.; Okan, B. S.; Menceloglu, Y. Z.; Yildiz, M. *RSC Adv.* **2016**, *6*, 9495-9506.
8. Zhang, H. B.; Zheng, W. G.; Yan, Q.; Jiang, Z. G.; Yu, Z. Z. *Carbon* **2012**, *50*, 5117-5125.
9. Guo, Z.; Ye, R.; Zhao, L.; Ran, S.; Fang, Z.; Li, J. *Compos. Sci. Technol.* **2016**, *129*, 123-129.
10. Li, K. Y.; Kuan, C. F.; Kuan, H. C.; Chen, C. H.; Liu, T. Y.; Chiang, C. L. *High Perform. Polym.* **2014**, *26*, 798-809.
11. Jiang, X.; Drzal, L. T. *Polym. Compos.* **2010**, *31*, 1091-1098.
12. Jiang, X.; Drzal, L. 41st International SAMPE Technical Conference (ISTC), 2009.
13. Asmatulu, R.; Khan, W. S.; Reddy, R. J.; Ceylan, M. *Polym. Compos.* **2015**, 36, 1565-1573.
14. Raji, A. R. O.; Varadhachary, T.; Nan, K.; Wang, T.; Lin, J.; Ji, Y.; Genorio, B.; Zhu, Y.; Kittrell, C.; Tour, J. M. *ACS Appl. Mater. Interfaces* **2016**, *8*, 3551-3556.
15. Okan, B. S.; Yürüm, A.; Gorgülü, N.; Gürsel, S. A.; Yürüm, Y. *Ind. Eng. Chem. Res.* **2011**, *50*, 12562-12571.
16. Gulmine, J. V.; Janissek, P. R.; Heise, H. M.; Akcelrud, L. *Polym. Test.* **2002**, *21*, 557-563.
17. Ferrari, A. C.; Meyer, J. C.; Scardaci, V.; Casiraghi, C.; Lazzeri, M.; Mauri, F.; Piscanec, S.; Jiang, D.; Novoselov, K. S.; Roth, S.; Geim, A. K. *Phys. Rev. Lett.* **2006**, *97*, 187401.
18. Sever, K.; Tavman, I. H.; Seki, Y.; Turgut, A.; Omastova, M.; Ozdemir, I. *Compos. Part B Eng.* **2013**, *53*, 226-233.
19. Inuwa, I.; Hassan, A.; Shamsudin, S. *Malaysian Journal of Analytical Sciences* **2014**, *18*, 466-477.
20. Bhattacharyya, A.; Chen, S.; Zhu, M. *Express Polym. Lett.* **2014**, *8*, 74-84.